

# Characterization of the Second Harmonic Signal from Collagen

Guy Cox\*<sup>a</sup>, Paul Xu<sup>b</sup>, Colin Sheppard<sup>b</sup>, John Ramshaw<sup>c</sup>

<sup>a</sup>Electron Microscope Unit; <sup>b</sup>School of Physics; University of Sydney, NSW 2006, Australia.

<sup>c</sup>CSIRO Molecular Science, 343 Royal Parade, Parkville, Vic 3052, Australia

## ABSTRACT

Collagen is known to be a very effective generator of the second harmonic of incident light from 700 to 1100nm, and second harmonic generation (SHG) microscopy is coming into use as a tool for studying the distribution of collagen in tissue. It also shows promise as a technique for characterising collagen - both in distinguishing different collagen types and their packing and in identifying degradation of collagen in pathologic conditions. However many aspects of image formation in SHG microscopy of collagen remain imperfectly understood, and we have commenced a rigorous study of these factors. The present paper presents the first results from this program.

**Keywords:** second harmonic generation, collagen, non-linear microscopy, 2-photon fluorescence, colocalization

## 1. INTRODUCTION

Recently the known property of collagen in generating the second harmonic from incident light has been applied as a high-resolution imaging tool, and shown to be one of the most precise and effective techniques for studying the distribution of collagen in a wide variety of tissue types<sup>1-4</sup>. Because a pinhole is not required, the full resolution improvement of a 'perfect' confocal microscope is available<sup>5,6</sup>, whereas in an actual confocal microscope this is always compromised by the finite size of the pinhole. This enables surprisingly high levels of resolution to be obtained in spite of the relatively long wavelength used for imaging (typically around 800nm). Resolution of 300nm or less, comparable with the length of a fibre-forming collagen molecule, has been shown in actual tissue samples<sup>2,3,5</sup>.

Collagen makes up about 6% of the vertebrate body; it is a vital constituent of bone, it is the major component of cartilage and tendons, and also plays an important structural rôle in skin, interstitial tissues and basal laminae. Over 20 different collagen types, each coded separately in the genome, have now been identified. These differ in certain amino acids which in turn affect the conformation of the triple-helical collagen molecule, so that the different collagen types have quite specific functions in the living organism. Types I, II, III and V form fibrils, while type IV forms sheets in basal laminae, and types VI and IX act as links, binding fibrillar collagen to other cell components. Type I is highly organised in fibrils, exhibiting a quasi-crystalline structure, and is very important as a structural component of bones, skin and tendons, but also occurs in many other tissues. Type II is the major collagen of cartilage and the vitreous humour of the eye<sup>7</sup>, while type III collagen is found in skin and blood vessels and a range of other extensible tissues.

In a previous paper<sup>3</sup> we have shown that SHG imaging appears to be able to distinguish between type I and type III collagen in tissue sections, both stained and unstained. SHG has also been used as a tool to detect the polarity of collagen in connective tissue<sup>8</sup> and this may also become applicable at higher resolution with current developments in instrumentation. Experimentally induced damage has been shown to affect the SH signal from collagen<sup>9</sup> and very recently pathologic changes have also been shown to be detectable by SHG properties<sup>10</sup>. Degradation of tooth collagen in dental caries is visible as a loss of the SHG signal<sup>11</sup>. Burn damage to collagen in skin also affects the SHG signal<sup>12</sup>. All these observations offer the promise of SHG microscopy becoming a valuable diagnostic tool, as do methods using SHG to measure collagen invasion in liver cirrhosis<sup>12,13</sup>.

Despite all this interest, there remain many aspects of the generation of second harmonics by collagen that are poorly

\* guy@emu.usyd.edu.au; phone +61 2 9351 3176; fax +61 2 9351 7682. <http://www-personal.usyd.edu.au/~cox/index.html>.  
Electron Microscope Unit F09, University of Sydney, NSW 2006 Australia

characterised, and this is a stumbling block to the widespread practical adoption of the technique. Experimental results on orientation dependence<sup>12</sup>, direction of propagation<sup>3</sup> and colocalisation<sup>15</sup> have been presented, but many questions remain unanswered. Even the question of direction of propagation is of interest, given that commercial instruments depending on backscattered SHG imaging are now reaching the marketplace<sup>15</sup>, yet the signal at the point of generation is almost exclusively propagated forwards<sup>3,16</sup>.

Key questions include:

1. To what extent are differences in SHG determined by the type of collagen and to what extent by the nature of the packing and the degree of crystallinity?
2. What are the effects of orientation and polarization on the signal?
3. To what extent is there any primary back-propagation of the signal, as opposed to secondary backscattering?

Our approach to answering these questions is to use pure and well-defined collagen samples, so that there are minimal confounding influences on the final signal. This paper presents the first results from this approach, as well as from well-characterised systems such as kangaroo-tail tendon.

## 2. MATERIALS AND METHODS

### 2.1 Collagen source

Calf skin was obtained from a local abattoir. Skin samples were un-haired by immersing in liquid nitrogen and brushing off the hair. The skin was then powdered while frozen. Mature bovine bones were obtained locally.

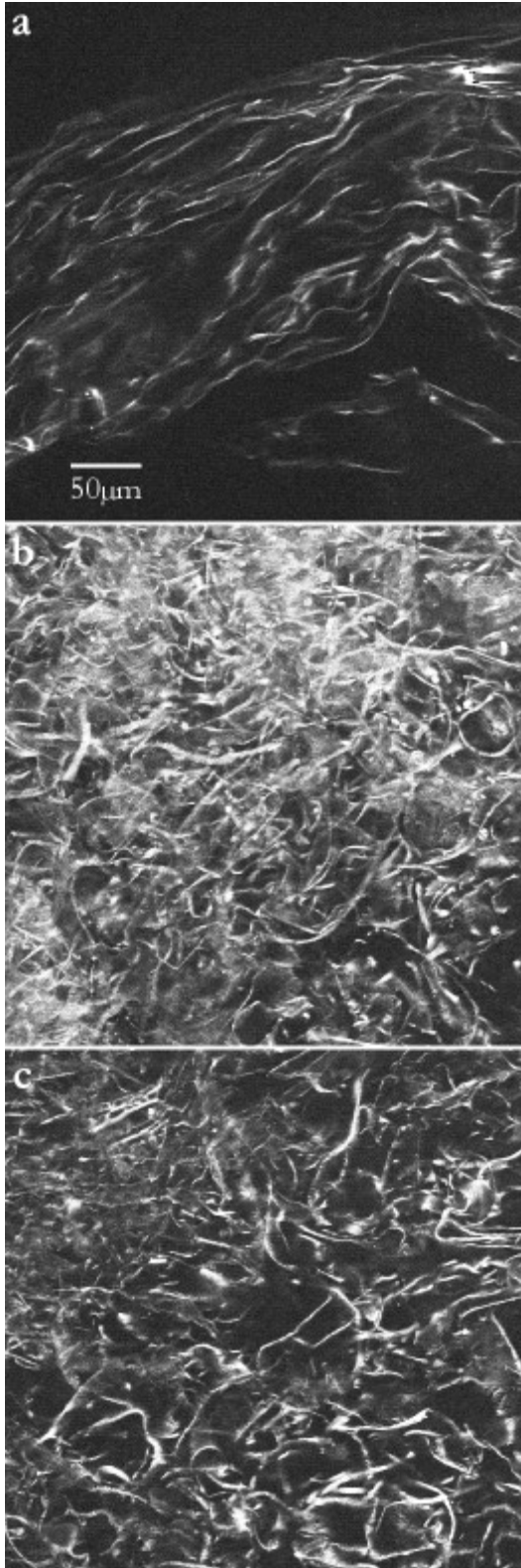
### 2.2 Collagen purification.

Powdered skin was suspended in 0.1 M acetic acid, adjusted to pH 2.5 with HCl, and solubilized by pepsin digestion, 1mg/ml enzyme, at 4°C for 48h. After removal of insoluble material by centrifugation, the soluble collagen was fractionated by NaCl precipitation<sup>17</sup>. At acid pH, the precipitate at 0.7 M NaCl, for types I and III collagens, was collected. This 0.7 M NaCl precipitate was further fractionated at pH 7.4, in 0.2 M Tris/HCl buffer, with precipitates at 1.7 M and 2.3 M NaCl being collected. The 2.3 M NaCl precipitate, which was type I collagen, was further purified by repeated precipitation using the same conditions.

The precipitate at 1.7 M NaCl, which contains both type I and type III collagens, was further fractionated by rapid ammonium sulphate fractionation, to 13% saturation<sup>17</sup>, to give a fraction enriched in type III collagen. Final purification of type III collagen was achieved by a cycle of denaturation in 4 M guanidine hydrochloride followed by renaturation by dialysis against water<sup>18</sup>.

For type II collagen, hyaline cartilage was dissected from mature bovine bone. Diced cartilage was suspended in 0.1 M acetic acid, adjusted to pH 2.5 with HCl, and solubilized by pepsin digestion, 1mg/ml enzyme, at 4°C for 120 h. After removal of insoluble material by centrifugation, the soluble collagen was fractionated by NaCl precipitation<sup>17</sup>. At acid pH, the precipitate at 0.7 M was collected, which contains type II collagen. The type II collagen was further purified by fractionation at pH 7.4, in 0.2 M Tris/HCl buffer. The precipitate at 2.5 M NaCl was removed, containing any type I collagen impurities that were present. Type II collagen was then collected by precipitation at 4.0 M NaCl.

After purification, all collagens were dialysed extensively against 25 mM acetic acid and were collected by freeze drying. Purity was examined by SDS-polyacrylamide gel electrophoresis<sup>19</sup>, with type I and III collagens separated using delayed reduction<sup>20</sup>. Small samples of the dried collagen were mounted in DPX mountant on slides under number 1.5 (0.17mm) coverslips.



### 2.3 Kangaroo tail tendon

Histological paraffin sections of glutaraldehyde-fixed kangaroo tail tendon samples, both unstained and stained with Sirius Red, were as used previously<sup>2,3</sup>.

### 2.4 Microscopy

The microscope used was a Leica DMIRBE inverted microscope, fitted with a Leica TCS-SP2 spectrometric confocal head (Leica Microsystems, Heidelberg, Deutschland). The laser is a Coherent Mira titanium sapphire system, tunable between 700nm and 1000nm, operating in the femtosecond regime and pumped by a 5W Verdi solid-state laser (Coherent Scientific, Santa Clara, Ca.). All additional detectors and optical equipment were supplied by Leica Microsystems, with the exception of the additional filters and dichroics, supplied by Chroma Inc (Brattleboro, Vt.) The setup was as described previously<sup>2,3</sup>, with the addition of a rotatable polariser between the condenser and the transmitted light detector. 830nm illumination was used with a 415/10nm detection barrier filter. Measurements were made either with the microscope software or with KS-Lite (Kontron Bild-Analyse, München, Deutschland).

### 2.5 Colocalization

Colocalization fluorograms were plotted using the built-in software of the Leica TCS-SP2 microscope, and with LaserPix software (Bio-Rad Ltd., Hemel Hempstead, UK). Numerical calculations of colocalization coefficients were carried out using LaserPix.

## 3. RESULTS

The purified Type I, II and III collagen samples were amorphous and therefore show the intrinsic SHG properties of the three collagen types without any confounding effects of sample packing and crystallinity. As expected, the SHG signal was much weaker than that seen in Type I collagen fibrils in tissue, and a relatively high laser power was needed to obtain adequate images. Figure 1 shows the appearance of the three collagen types. All were taken at the same photomultiplier setting and laser (EOM) setting, and it is clear (and numerical measurements confirm) that there is no significant difference between them.

There was significant autofluorescence from these samples, in a broad band of the spectrum between ~550nm and 650nm. The native autofluorescence of ordered type I collagen in tendons is

**Figure 1.** Purified, amorphous collagen mounted in DPX, imaged with x40 NA 0.75 dry lens. PMT gain and EOM setting were identical for all 3. (a) Type I collagen; (b) Type II collagen; (c) Type III collagen.

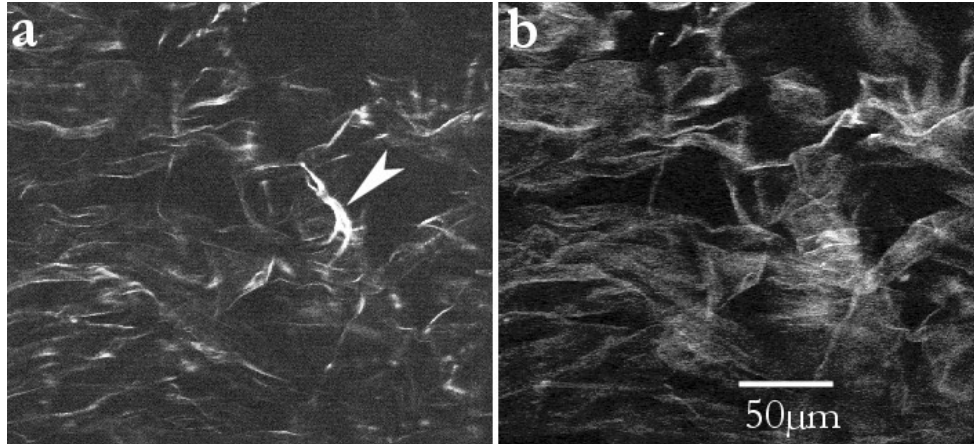


**Figure 2.** Purified type I collagen excited at 830nm. (a) SHG signal at 415nm (b) autofluorescence detected between 450 and 650nm. Arrowhead indicates a fragment which is generating a strong SH signal but shows no autofluorescence

seen at  $\sim 590\text{nm}^{21}$  (excitation at 355nm), which could not be excited by two-photon excitation at 830nm. The autofluorescence of the three amorphous collagen samples could possibly result from residual parts of cross-links that remain during the purification process. Figure 2 shows the second harmonic image and corresponding autofluorescence image of purified type I collagen. While the images are broadly comparable, one particular collagen fragment (arrowed) gives a particularly strong second-harmonic signal but no visible autofluorescence. This may be a small zone where the purified collagen has re-formed into an ordered fibril-like aggregate.

In the highly-ordered collagen of kangaroo tail tendon we have noted<sup>3</sup> that there is not an exact colocalization between fluorescence (whether autofluorescence or stain) and the SHG signal. Therefore fluorescence/SHG correlation coefficients were measured for both purified collagen and stained and unstained tendon samples. Colocalization plots (fluorograms) are shown in Figure 3, and numerical results in Table 1.

Sample	COLOCALISATION COEFFICIENTS	
	Fluorescence - SHG	SHG - Fluorescence
KTT - stained Sirius Red	0.034	0.214
KTT - unstained (aldehyde fixed)	0.102	0.913
Pure, amorphous Type I	0.512	0.431
Pure amorphous Type II	0.791	0.623
Pure amorphous Type III	0.761	0.371

**Table 1** - Colocalization coefficients between fluorescence and second harmonic signals for 5 different collagen samples.

These results show that there was a strong degree of colocalization in all cases. This was weakest in the case of Sirius Red, where the fluorescence can be attributed to both the stain and autofluorescence. In both the kangaroo tail samples the correlation between SHG and fluorescence was much stronger (by nearly an order of magnitude) than vice versa, showing that while most regions generating the second harmonic were also fluorescent, there were many regions which were fluorescent but showed no harmonic signal. In contrast, in the pure, amorphous collagen samples the correlations were much more equal in both directions, though overall the fluorescence - SHG correlation was the stronger, implying that most of the sample generated the second harmonic but only part was fluorescent.

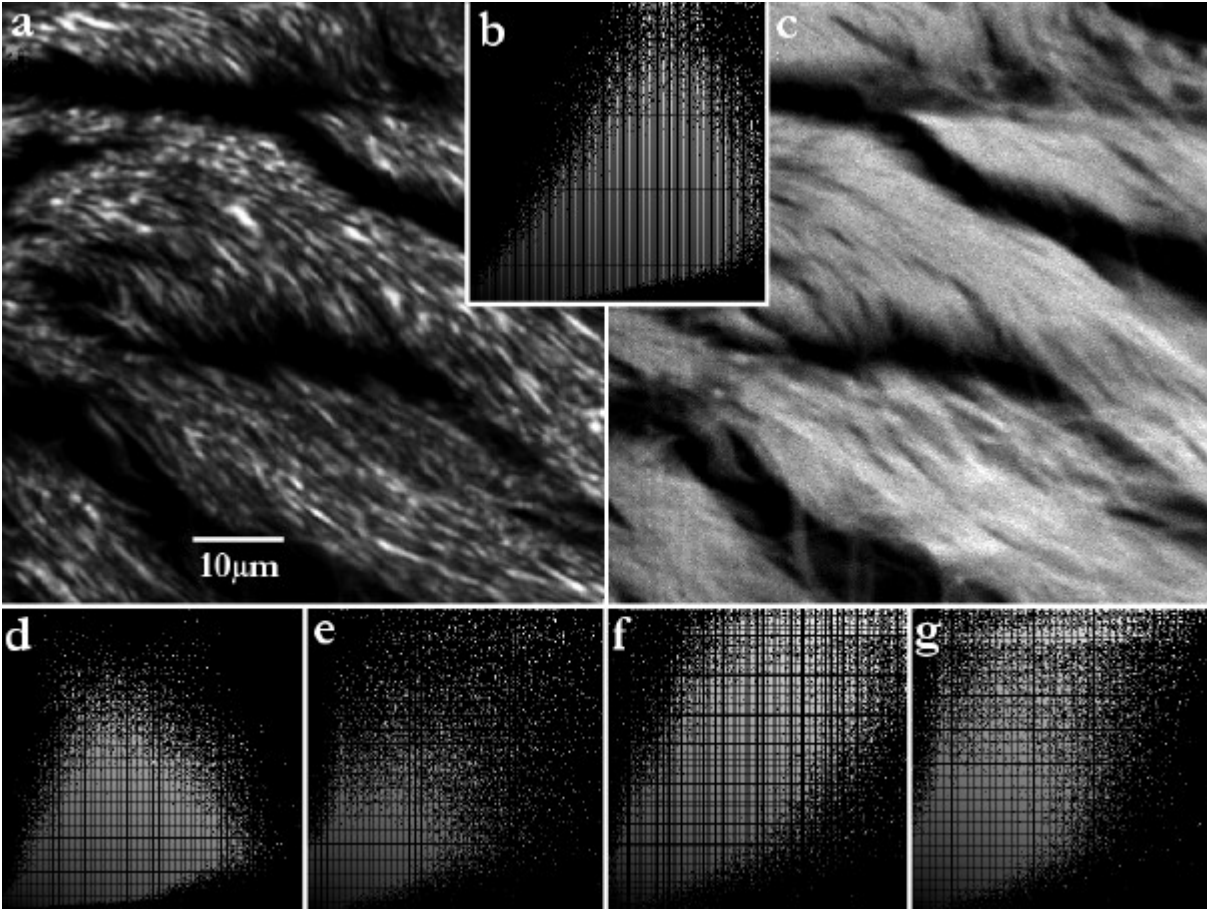


**Figure 3.** Colocalization between fluorescence and second harmonic signals. (a) & (c) SHG image from histological section of fixed, unstained kangaroo-tail tendon and corresponding fluorescence image. (b) colocalization diagram from a & c. (d - e) Colocalization fluorograms. (d) Sirius red stained kangaroo-tail tendon (e) Purified type I collagen (f) Purified type II collagen (g) Purified type III collagen. In all the fluorograms Y-axis represents SHG intensity and X axis represents fluorescence intensity. All images were scaled to a contrast range of 0-255 - dark lines in the fluorograms represent missing intensities resulting from the scaling.

In amorphous collagen the individual molecules should be randomly aligned, and hence polarization properties should not be determined by fibril orientation. We investigated the polarization of the second harmonic signal by placing a rotatable polarizer close to the plane of the condenser iris. The initial plane of polarization of the beam was established by removing both the sample and the filter block and setting the polarizer for maximum transmission of the incoming beam.

Figure 4 shown the images obtained. With both type I and type II collagen a very weak signal was seen with the analyser parallel to the polarization of the incident beam. The signal was quite clearly at its strongest with the polariser set at 90° to the incoming polarization. The images were segmented to identify regions of collagen, selecting intensities of 30 and above in the 90° image to avoid the background. The same segmentation mask (smoothed and hole-filled) was used for all 4 images in each series so that exactly the same pixels were measured in each case. The mean intensity for the segmented region was obtained, as well as the intensities and areas of each individual segmented item. The mean intensities are shown in Table 2. In both cases the mean intensity more than doubles at 90° compared to the 0° value.

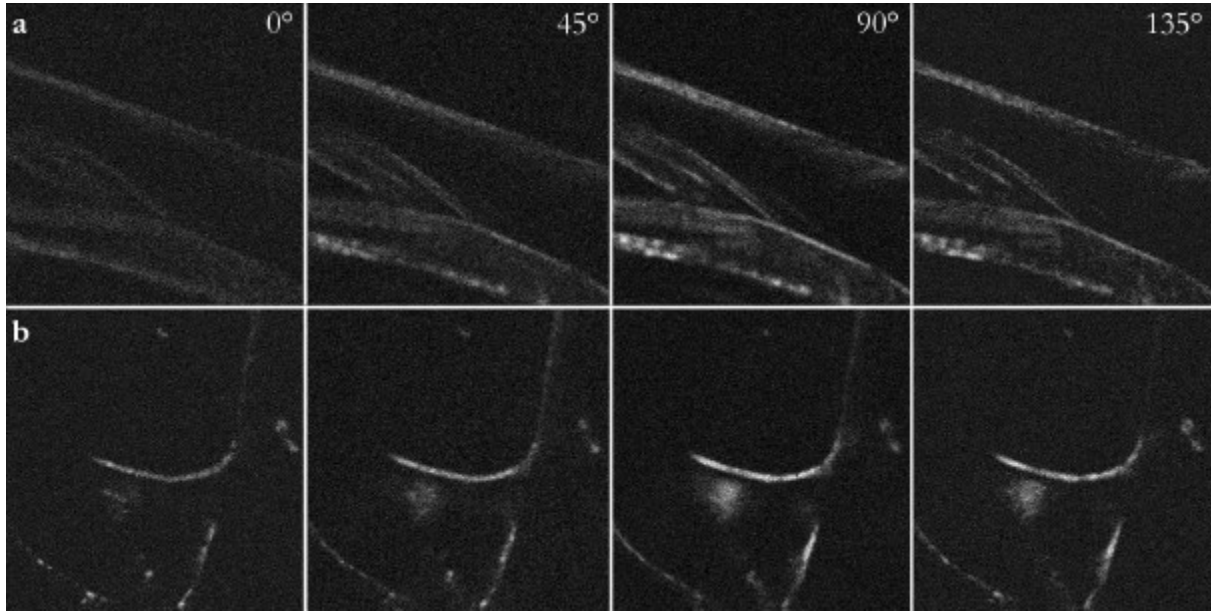


**Figure 4.** Images of (a) type I collagen and (b) type II collagen. Each row presents the same field, with the polariser at the specified angle to the incoming beam. Intensities have been scaled and a gamma correction applied to make the dimmer features visible - the same scaling and correction were applied to all images.

Sample	POLARISER ANGLE			
	0°	45°	90°	135°
Type I	19.8	30.1	45.6	35.7
Type II	32.6	44.3	68.7	56.3

**Table 2.** Mean intensities for the collagen aggregates seen in Figure 4. (Mean of the whole masked area).

Direction of signal propagation was measured on both lightly covered slides (approximately 50% coverage with collagen aggregates) and on slides with a dense mat of collagen (> 100% coverage). As for the polarization experiment, the collagen aggregates were segmented out, and the same segmentation mask was used for both images (epi and dia). Mean intensity for the segmented area was measured using the KS-Lite software. Results are shown in Table 3. In the low-density slides the epi-detector image was barely visible on screen. We have found<sup>3</sup> that the epi-detector shows about 50% of the sensitivity of the transmitted one at equivalent photomultiplier voltage and the results were therefore corrected for that. In the thinnest sample only 14% of the total signal propagated backwards, but the proportion rose dramatically with thicker specimens, to 80% with a dense mat of collagen.

Sample	Cover (%)	Dia	Epi (raw)	Epi (corrected)	Epi / Dia
Type III	49.6	143	11.6	23.2	0.16
Type III	>100	28.4	56.9	113.8	4.01
Type II	66	131	19.9	39.8	0.3

**Table 3.** Mean intensities in transmitted (dia) and back-propagated (epi) direction for three different collagen samples. The cover is the proportion of the total area covered by the segmented objects and makes no allowance for overlap, which was substantial. The entire area was measured for the very densely covered sample.

#### 4. DISCUSSION

These results show that there is little, if any difference in the intrinsic second-harmonic generating capability of the three types of collagen studied here. The huge differences observed in tissue must be attributed to the different degrees of packing and crystallinity they exhibit *in vivo*. These types, I, II and III, are all fibrillar collagens and it would be interesting to see if the same held true of non-fibrillar collagens. The amorphous bovine collagen samples, which were extracted from mature tissue, showed an autofluorescence which is absent from tendon collagen in its native state<sup>21</sup>. It is also absent from regions in purified collagen which show strong second harmonic generation. Our future plans include re-forming fibrils with their quasi-crystalline structures from these purified collagens; we hope that it will then be possible to correlate the degree of order and crystallinity with the second harmonic signal.

The colocalization experiments support the idea that the bulk of the SHG signal in a tissue sample comes from highly ordered and densely packed collagen. Differing statements in the literature clearly call for a more rigorous, numerical investigation of colocalization, since it has been claimed both that the SHG and TPF signal do colocalise<sup>14</sup>, and that there is (at high resolution) not a precise colocalization<sup>2,3</sup>. Fortunately a rigorous approach to colocalization, based on Pearson's correlation coefficient, has been described<sup>22</sup>. This defines two colocalization coefficients,  $M_1$  and  $M_2$  as:

$$M_1 = \frac{\sum_i F_{i,coloc}}{\sum_i F_i} \quad (1)$$

$$M_2 = \frac{\sum_i S_{i,coloc}}{\sum_i S_i} \quad (2)$$

where  $F_i$  and  $S_i$  are pixel intensities in fluorescence and second harmonic respectively.  $F_{i,coloc} = F_i$  if  $S_i > 0$  and  $F_{i,coloc} = 0$  if  $S_i = 0$ ;  $S_{i,coloc} = S_i$  if  $F_i > 0$  and  $S_{i,coloc} = 0$  if  $F_i = 0$ .  $M_1$  and  $M_2$  are robust coefficients which have been shown to be useful even where there are substantial differences in intensity between the two signals<sup>22</sup>.

All the images investigated show strong colocalizations between the harmonic and fluorescence signals. Since all proteins are fluorescent after aldehyde fixation, it is to be expected that in the samples of native tissue the correlation coefficients show a substantial amount of fluorescence which is not associated with the second harmonic. It may seem surprising, though that there is more fluorescence which is independent of the harmonic signal in the sample stained with Sirius Red, a collagen-specific dye. Areas known to contain type III collagen<sup>3</sup> were excluded from the images analysed. However there remains the possibility that types VI and IX are present in the tendon, and these would stain with Sirius Red but, since they are not crystalline, not give a strong SHG signal.

According to Stoller et al.<sup>12</sup>, SHG appears strongest while the fibrils of the collagen are in parallel with the E field of the incident beam. In our purified sample there are no true fibrils, so we can assume that in principle all orientations are present. Since collagen molecules are quite long in relation to the size of the smallest aggregates seen in our images there does exist the possibility that they could become co-aligned to some extent in these aggregates. However, in general the images (Figures 1, 3 & 4) do not show any strong tendency for aggregates in one direction to be brighter than aggregates aligned at right angles to them. This suggests that most aggregates contain all molecular orientations.

On the other hand, the second harmonic polarization was also assumed by Stoller et al.<sup>12</sup> to have the same orientation as the axis of the fibrils. If this were so, in our experiment we should expect the SHG to be strongest while the polarizer is set to 0°. The result however, showed the contrary: we receive most signal at around 90° and almost none at 0°. All parts of the images of type I are fairly consistent in this regard; in all 22 segmented aggregates the ratio 90°/0° ranges from 1.4 to 3.1, with a mean of 2.3, and all show a minimum at 0° and a maximum at 90°. The sample of type II, as a glance at Figure 4b will show, does not behave in the same uniform way. Even though the overall trend is identical,

some small regions behave differently. The  $90^\circ/0^\circ$  ratios vary between 0.74 and 2.9; two small regions have maxima at  $45^\circ$  and minima at  $135^\circ$ . These are only small aggregates, and the most probable explanation is that in these the collagen molecules show a relatively high degree of alignment so that molecular orientation effects predominate - with no molecules in the most favourable position for excitation we see instead the radiation from the orientation that is present. A more detailed study of this phenomenon is being planned.

The directionality of the signal has also been an issue, with several published studies<sup>14,15,23</sup> which have measured back-propagated second harmonic signals. Our results on purified collagen are still preliminary, but they show that in thin samples propagation is strongly in the forward direction, and as the sample becomes thicker more backscattered SH signal is seen. Eventually, with a thick enough sample the combination of backward scattering and attenuation of the forward-propagated signal can make the back-propagated signal stronger than the forward one (Table 3). This supports our view, based on both experimental observation<sup>3</sup> and theoretical predictions<sup>16</sup>, that the SHG signal from collagen, at the point of generation, propagates virtually exclusively forward. Back-propagated signal is the result of diffuse scattering, but can nevertheless be strong enough to be practically useful. However, since it is diffuse it will not be detectable in a confocal detection system, and this also matches our experimental results.

## 5. CONCLUSIONS

This study represents the first comprehensive attempt to fully characterise the SHG signal from collagen, in order to develop practical and useful clinical imaging modalities. The results presented here are preliminary, but they show that much of the observed differences in signals from different collagen types in tissue result from the different packing of collagen molecules rather than the second harmonic generating properties of the different types of collagen molecules as such. We plan to extend this work by reconstituting structured fibrils from the amorphous collagen and also by looking at non-fibril forming collagen types. With such samples we should be able to further elucidate the clearly complex relationship between stains such as Sirius Red and SHG.

The use of amorphous collagen has enabled some novel insights, particularly the surprising observation that the second harmonic is preferentially polarised at right angles to the incoming beam. This also needs much further investigation but it could have interesting consequences for determination of collagen orientation and polarity in tissue. The second harmonic from amorphous collagen propagates forwards, as in thin tissue sections, so that ordered geometry is not a requisite for this. However, a sufficiently bulky sample will scatter much of the harmonic signal backwards.

## ACKNOWLEDGEMENTS

The purchase of the microscope described here was funded in part by Australian Research Council Research, Infrastructure, Equipment and Facilities grant R00002784. We thank Dr Allan Jones for the kangaroo tail samples. Some of this work was funded by Australian Research Grant No. DP0210312 to CS & GC.

## REFERENCES

1. P. Campagnola, H.A. Clark, W.A. Mohler, A. Lewis and L.M. Loew. "Second-harmonic imaging of living cells." *Journal of Biomedical Optics* **6**, 277-286, 2001
2. G.C. Cox, F. Anconi, and E. Kable, "Second harmonic imaging of collagen in mammalian tissue." *Proceedings of SPIE* **4620**, 148-156, 2002
3. G. Cox, E. Kable, A. Jones, I. Fraser, F. Manconi and M. Gorrell "3-dimensional imaging of collagen using second harmonic generation." *Journal of Structural Biology*, in press. 2002
4. P.J. Campagnola, A.C. Millard, M. Terasaki, P.E. Hoppe, C.J. Malone and W.A. Mohler, "Three-dimensional high-resolution second-harmonic generation imaging of endogenous structural proteins in biological tissues." *Biophysical Journal* **81**, 493-508. 2002



5. G. Cox, E. Kable, C.J.R. Sheppard, P. Xu. "Resolution of second harmonic generation microscopy." *Proceedings 15th International Congress of Electron Microscopy* **2**, 331-332, 2002
6. R. Gauderon and C.J.R Sheppard, "Two-dimensional weak-object transfer functions in the scanning harmonic microscope." *Journal of Modern Optics* **47**, 1195-1202, 2000
7. H. Lodish, A. Berk, S.L. Lipursky, P. Matsudaira, D. Baltimore and J. Darrell. *Molecular Cell Biology* (4th Edition) W.H. Freeman & Co, New York, 2000
8. Freund I., Deutsch M. and Sprecher A., "Connective tissue polarity. Optical second-harmonic microscopy, crossed-beam summation, and small-angle scattering in rat-tail tendon." *Biophysical Journal* **50**, 693-712, 1986
9. Kim B.M., Eichler J., Reiser K.M., Rubenchik A.M. and Da Silva L.B. "Collagen structure and nonlinear susceptibility: effects of heat, glycation, and enzymatic cleavage on second harmonic signal intensity." *Lasers in Surgery and Medicine* **27**, 329-35, 2000.
10. Deng, X., Williams E.D., Thompson E.W., Gan X. and Gu M. "Second harmonic generation from biological tissues: effect of excitation wavelength." *Scanning* **24**, 175-178, 2002
11. Swain, M and Mahoney, E., in preparation, 2003
12. Stoller, P., Celliers, P.M., Reiser, K.M. and Rubenchik, A.M. "Imaging collagen orientation using polarization-modulated second harmonic generation." *Proceedings of SPIE* **4620**, 157-165, 2002
13. M. D. Gorrell, X M. Wang, M T. Levy, E Kable, G Marinos, G Cox and Geoffrey W. McCaughan. "Intrahepatic expression of collagen and fibroblast activation protein (FAP) in hepatitis c virus infection." In: *Dipeptidyl aminopeptidases in health and disease*. Kluwer Academic/Plenum Publishers New York, U.S.A., 2003
14. A. Zoumi, A.T. Yeh and B.J Tromberg. "Combined two-photon excited fluorescence and second harmonic generation backscattering microscopy of turbid tissues." *Proceedings of SPIE* **4620**, 175-181, 2002
15. K. König, U. Wollina, I.Riemann, C. Peukart, K-J. Halbhuber, H. Konrad, P. Fischer. V. Fünfstück, TW. Fischer, and P. Elsner. "Optical tomography of human skin with subcellular spatial and picosecond time resolution using intense near-infrared femtosecond laser pulses." *Proceedings of SPIE* **4620**, 191-201, 2002
16. G. Cox and E. Kable. "Second harmonic imaging of collagen." In: *Cell Imaging Techniques* (ed. D. Taatjes). Humana Press, 2003.
17. R.L. Trelstad, V.M. Catanese and D.F Rubin. "Collagen fractionation: separation of native types I, II and III by differential precipitation." *Analytical Biochemistry* **71**, 114 -118, 1976.
18. J. ChandraRajan. "Separation of type III collagen from type I collagen and pepsin by differential denaturation and renaturation." *Biochemical and Biophysical Research Communications*. **83**, 180-186, 1978.
19. U.K. Laemmli. "Cleavage of structural proteins during the assembly of the head of bacteriophage T4." *Nature (London)* **227**, 680-685, 1970
20. B. Sykes, B. Puddle, M. Francis and R. Smith. "The estimation of two collagens from human dermis by interrupted gel electrophoresis." *Biochemical and Biophysical Research Communications*. **72**, 1472-1480, 1976
21. T. Theodossiou , E. Georgiou, V. Hovhannisyan, K. Politopoulos and D. Yova., "Energy transfer between collagen-dye molecules as a probe of higher-lying electronic states following multiquantum excitation" *Journal of Optics A: Pure and Applied Optics* **3** L1-L3, 2001
22. E.M.M. Manders, F.J. Verbeek and J.A. Aten. "Measurement of co-localization of objects in dual-colour confocal images." *Journal of Microscopy* **169**, 375-382, 1993
23. E. Georgiou, T. Theodossiou , V. Hovhannisya, K. Politopoulos, G.S. Rapti, D. Yova., "Second and third optical harmonic generation in type I collagen, by nanosecond laser irradiation, over a broad spectral region" *Optics Communications* **176** , 253-260, 2000.